Biosensors and Bioelectronics 41 (2013) 309–315

Contents lists available at SciVerse ScienceDirect

Biosensors and Bioelectronics

journal homepage: www.elsevier.com/locate/bios

Direct electrochemistry of glucose oxidase at electrochemically reduced graphene oxide-multiwalled carbon nanotubes hybrid material modified electrode for glucose biosensor

Veerappan Mani, Balamurugan Devadas, Shen-Ming Chen*

Electroanalysis and Bioelectrochemistry Lab, Department of Chemical Engineering and Biotechnology, National Taipei University of Technology, No.1, Section 3, Chung-Hsiao East Road, Taipei 106, Taiwan, ROC

ARTICLE INFO

Article history:
Received 3 July 2012
Received in revised form
13 August 2012
Accepted 20 August 2012
Available online 28 August 2012

Keywords:
ERGO–MWCNT hybrid
Glucose oxidase
Direct electrochemistry
Amperometry
Practicality

ABSTRACT

Direct electrochemistry of glucose oxidase (GOx) at an electrochemically reduced graphene oxide–multiwalled carbon nanotubes hybrid (ERGO–MWCNT) modified glassy carbon electrode (GCE) has been reported. The π–π stacking interaction operating between the MWCNT and graphene oxide (GO) has been revealed by UV–Vis absorption spectroscopy. GOx was well immobilized onto the ERGO–MWCNT hybrid film, as a result direct electrochemistry of GOx has been achieved. Compared with pristine MWCNT, 2.1 fold higher peak current and very low peak to peak separation (ΔE_p) of 26 mV were observed at the hybrid film, demonstrating faster electron transfer between GOx and the modified electrode surface. Moreover, the modified film exhibited high electrocatalytic activity towards glucose via reductive detection of oxygen consumption and in the presence of mediator. The proposed biosensor exhibits low detection limit of 4.7 μM with wide linear range of 0.01–6.5 mM and acquires excellent storage and operational stabilities. The accurate glucose determination in human blood serum and good recoveries achieved in spiked urine samples revealed their great potential in the practical applications.

1. Introduction

Graphene, a monolayer of sp^2 bonded carbon atoms with versatile electronic, mechanical and thermal properties has been emerged as a promising material in diverse fields of research. Owing to its interesting physicochemical properties, it finds wide range of applications including electronics, super capacitors, batteries, fuel cells and biosensors (Geim and Novoselov, 2007; Pumera et al., 2010; Yoo et al., 2008). Although graphene can be prepared by several methods, most of them are not suitable for mass production and processing, which limit its applications (Chen et al., 2010). One viable method for the bulk production of graphene is chemical method, involving chemical oxidation of graphite to graphene oxide (GO) and subsequent reduction (Hummers and Offeman, 1958). GO, the oxygenated derivative of graphene is an amphiphilic molecule, in which hydrophilicity makes it highly dispersible in water, whereas hydrophobicity provides active sites for the interaction with other aromatic compounds (Dreyer et al., 2010).

On the other hand, carbon nanotube (CNT) viewed as a rolled graphene sheets also exhibits excellent mechanical, electrical and electrocatalytic properties (Wang, 2005). In the past decade, massive amount of works have been done on both multiwalled carbon nanotube (MWCNT) and single walled carbon nanotube (SWCNT) based electrochemical sensors and biosensors (Jacobs et al., 2010). Although, it can be easily dispersed in organic solvents, it tends to irreversible agglomeration in a short period of time because of Van der Waals interactions between the side walls. To overcome this shortcoming, several strategies have been developed in the past using surfactants, ionic liquids, polymer wrapping and chemical functionalization approaches (Kachoosangi et al., 2009; Kang and Taton, 2003). But still, a thirst to explore a better dispersant for MWCNT is everlastingly increasing among the researchers.

Being a versatile dispersant, GO has a unique ability to form stable aqueous dispersions, highly bio-compatible and possess good electrocatalytic properties (Ramesha and Sampath, 2007). In addition, its reductive product graphene is a unique material with potential applications in diverse fields and one of the hottest materials of interest. Zhang et al. (2010) demonstrated that it is possible to prepare a water dispersible GO-MWCNT hybrid material via non-covalent π–π stacking interactions. Dispersing MWCNT via non-covalent approaches cannot depress its intrinsic

* Corresponding author. Tel.: +886 2270 25238; fax: +886 2270 17147.
E-mail address: smchen78@ms15.hinet.net (S.-M. Chen).

0956-5663/$ - see front matter © 2012 Elsevier B.V. All rights reserved.
http://dx.doi.org/10.1016/j.bios.2012.08.045

electrical, mechanical, and optical properties. The incorporation of GO with MWCNT render this hybrid material as a versatile platform for the electrocatalytic applications. Conversely, the insulating property of GO caused by the aliphatic sp^3 hybridized domain, limits its conductivity. Therefore for improving the conductance, it can be reduced to graphene either by chemical, thermal or electrochemical methods (Gao et al., 2010). Often chemical methods involve the use of highly toxic reductant hydrazine (Mani et al., 2012), whereas thermal methods require high temperatures. On the other hand, electrochemical approach involved neither toxic reducing agents nor high temperature, rather considered to be versatile, fast, efficient and green. Recent studies as well reveal that the electrochemical reduction of GO to graphene was appreciably improved after the incorporation of MWCNT (Qiu et al., 2010).

Acute monitoring of glucose is of significant importance and it has been successively achieved by using GOx based biosensors. Till now, numerous approaches have been developed for the GOx immobilization based on CNT modified electrodes. Some of the reported literature including CNT-gold colloid modified electrode (Yao and Shiu, 2008), gelatin-MWCNT (Periasamy et al., 2011), polymerized ionic liquid-wrapped CNT (Xiao et al., 2010), CNT-ionic liquid composite (Kachoosangi et al., 2009), nitrogen doped MWCNT (Deng et al., 2009), MWCNT–GOx (Gutierrez et al., 2012) and boron-doped CNT (Deng et al., 2008). Other than CNTs, several strategies were employed for the GOx immobilization based on graphene based modified electrodes. These approaches include polyvinyl pyrrolidone-protected graphene/polyethylenimine-functionalized ionic liquid (Shan et al., 2009), graphene-Au-nafion biocomposite (Zhou et al., 2010), nitrogen-doped graphene (Wang et al., 2010), GOx–graphene–chitosan (Kang et al., 2009) and chitosan–ferrocene/GO (Qiu et al., 2012).

In this report, for the first time we exploited ERGO–MWCNT hybrid material for the effective immobilization of GOx and studied its direct electrochemistry. Furthermore, the prepared modified electrode has been demonstrated as a versatile glucose biosensor. The accurate glucose determination achieved in human blood serum and spiked urine samples were proved the great ability of the sensor in the practical applications.

2. Experimental

2.1. Reagents and apparatus

GOx, type x–s from aspergillus Niger, graphite (powder, $< 20\ \mu m$), MWCNT (bundled $> 95\%$, O.D × I.D × length of 7–15 × 3–6 × 0.5–200 μm) were purchased from Sigma-Aldrich and used as received. 5 wt% nafion (Nf) was purchased from Aldrich and the required Nf concentrations were prepared in definite volume of ethanol. The mediator ferrocene mono carboxylic acid (FMCA) was purchased from Alfa Aesar. All the reagents were of analytical grade and used without purification. The supporting electrolyte used for the electrochemical studies was 0.1 M phosphate buffer solution (PBS), prepared using Na_2HPO_4 and NaH_2PO_4 and the pH was adjusted either using H_2SO_4 or NaOH. Prior to each experiment, all the solutions were deoxygenated with pre-purified N_2 gas for 15 min unless otherwise specified.

The electrochemical measurements were carried out using CHI 611A work station. Electrochemical studies were performed in a conventional three electrode cell using BAS GCE as a working electrode (area 0.07 cm^2), saturated Ag/AgCl as a reference electrode and Pt wire as a counter electrode. Amperometric measurements were performed by an analytical rotator AFMSRX (PINE instruments, USA) with a rotating disc electrode (RDE) having working area of 0.24 cm^2. UV–Vis absorption and Fourier transform infrared (FT-IR) spectroscopic measurements were carried out using Hitachi U-3300 spectrophotometer and Perkin Elmer spectrum RXI, respectively. EIM6ex ZAHNER (Kroanch, Germany) was used for electrochemical impedance spectroscopy (EIS) studies. Field emission scanning electron microscopy (FESEM) was performed using JEOL JSM-6500F.

2.2. Preparation of GO–MWCNT hybrid material

Graphite oxide was synthesized by modified Hummer's method (Hummers and Offeman, 1958) and it was exfoliated through ultrasonication for 2 h to get graphene oxide (GO). The as-obtained aqueous GO solution was subjected to centrifugation for 30 min at 4000 rpm to remove any unexfoliated graphite oxide. Thereafter, 5 mg of MWCNT was added into 10 mL of GO solution (0.5 mg mL^{-1}) and the mixture was subjected to ultrasonication for 2 h. An unstabilized MWCNT and excess of GO were removed by subjecting two consecutive centrifugation cycles (30 min each) at 8000 and 14,000 rpm, respectively, and the residue was assigned to be GO–MWCNT hybrid (Zhang et al., 2010). Thus obtained hybrid material was dried overnight, re-dispersed in water (0.5 mg mL^{-1}) and used for further studies. The dispersion is highly stable for more than 6 months. As a control, GO and pristine MWCNT dispersions (0.5 mg mL^{-1}) were prepared in water and DMF solvents, respectively.

2.3. Fabrication of ERGO-MWCNT /GOx/Nf modified GCE

GCE surface was polished with 0.05 μm alumina slurry using a Buehler polishing kit, then washed with water, ultrasonicated for 5 min and dried. 5 μL of GO–MWCNT dispersion was drop casted onto the pre-cleaned GCE and dried at room temperature. Thereafter, GO–MWCNT modified GCE was transferred to an electrochemical cell containing 0.1 M PBS (pH 5). The GO–MWCNT was electrochemically reduced by performing 3 consecutive cyclic voltammograms briefly explained in the Section 3.2. Then 4 μL (10 mg mL^{-1}) of GOx was spread gently onto the surface of ERGO–MWCNT modified GCE and dried at ambient temperature. The GOx modified surface was smoothly washed with water to remove loosely adsorbed enzyme. Finally 2 μL (0.5%) of Nf was drop casted and the fabricated ERGO–MWCNT/GOx/Nf film modified GCE was dried. For comparison, ERGO/GOx/Nf and MWCNT/GOx/Nf modified GCEs were prepared by adopting the similar procedures.

3. Results and discussion

3.1. Characterization of as synthesized ERGO–MWCNT

The FESEM image of the GO–MWCNT hybrid film at 100 nm resolution is shown in Fig. 1A. It can be seen that thin GO sheets were completely wrapped onto the tubular network of MWCNTs. The possible interaction is π–π stacking interaction between the hydrophobic region of GO and the sidewalls of MWCNT. This interaction avoids the restacking of MWCNT and keeps the GO–MWCNT dispersion stable for long time. Further, UV–Vis absorption spectroscopy has been used to confirm the π–π interactions involved between GO and MWCNT. Fig. 1B depicts the UV–Vis spectra of GO (a) and GO-MWCNT (b). The UV–Vis spectrum of GO exhibits two characteristic absorption peaks. A broad absorption peak at 229 nm assigned to π–π^* transition and a shoulder peak at 280 nm assigned to n–π^* transitions. Interestingly, the π–π^* transition of GO appeared at 229 nm was red shifted to higher wavelength of 248 nm (Bathochromic Shift) in the spectrum of GO-MWCNT. Hence, the interaction should be π–

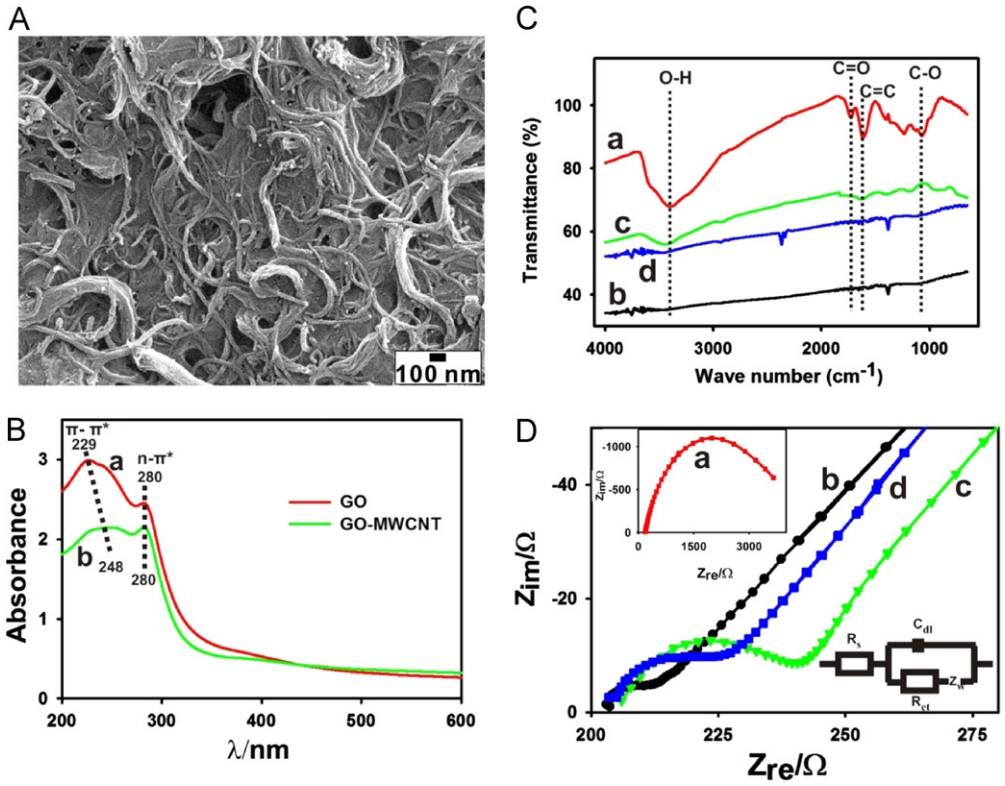

Fig. 1. (A) FESEM image of GO–MWCNT. (B) UV–Vis absorption spectra of GO (a) and GO–MWCNT (b). (C) FTIR spectra and (D) EIS of GO (a), MWCNT (b), GO–MWCNT (c) and ERGO–MWCNT (d). Inset: randles equivalent circuit model.

π stacking interaction between the aromatic basal plains of GO and MWCNT. Besides, no noteworthy shift has been observed for the n–π^* transition. Thus, UV–Vis spectra confirm that the interaction between GO and MWCNT is non-covalent π–π stacking interaction via hydrophobic aromatic regions of GO and that of MWCNT (Zhang et al., 2010).

Fig. 1C shows the FTIR spectra of GO (curve *a*) which displays well-defined characteristic peaks, ν(C–O)=1040 cm^{-1}, ν(C–C)=1620 cm^{-1}, ν(C–O)=1729 cm^{-1} and ν(–OH)=3318 cm^{-1}, ascribed to the stretching vibrations of the typical oxygen functionalities of GO. Whereas, no such characteristic peaks were observed for MWCNT (curve *b*). Interestingly, the FTIR spectra of MWNT-GO hybrid material (curve *c*) exhibited all the characteristic peaks described for GO though appear with less intense. Apparently, these peaks were appeared because of the co-existance of GO along with MWCNT in the hybrid. Moreover, all the peaks were disappeared in the spectra of ERGO–MWCNT (curve *d*), indicating the significant reduction of the aforementioned oxygen functionalities upon electrochemical reduction. Thus FTIR results also confirms the formation of GO–MWCNT and its reduction.

Fig. 1D shows the real and imaginary part of the EIS spectra represented as Nyquist plots (Z_{im} vs. Z_{re}) for GO (above inset to Fig. 1D, curve *a*), MWCNT (b), GO–MWCNT (c) and ERGO–MWCNT (d) modified GCEs using 5 mM $Fe(CN)_6^{3-/4-}$ as the electrolyte. Randles equivalent circuit model has been used to fit the experimental data where, R_s is electrolyte resistance, R_{et} is charge transfer resistance, C_{dl} is double layer capacitance and Z_w is Warburg impedance (Fig. 1D, below inset). EIS of the GO shows an enlarged semicircle than that of other modified films, owing to the insulating property of GO. On the other hand, MWCNT exhibits small semicircle; apparently because of the rapid electron transfer attributed to the excellent conductivity of MWCNT. Interestingly, GO–MWCNT modified GCE also exhibits a smaller semicircle than that of GO modified GCE. It clearly indicates that MWCNT was firmly attached to the GO surface which facilitates the conductivity of GO–MWCNT hybrid material. On the other hand, ERGO–MWCNT modified GCE exhibits much smaller semicircle indicating that the conductivity has been significantly improved upon electrochemical reduction. Thus, the EIS results also support the formation of the hybrid material.

3.2. Electrochemical reduction of GO-MWCNT

Fig. 2A shows the electrochemical reduction of GO–MWCNT hybrid at the potential range from 0 to −1.5 in PBS (pH 5). During the first cycle, a large cathodic peak appeared at −1.1 V (onset potential of −0.3 V) could be due to the reduction of oxygen functional groups such as hydroxyl, epoxy and carboxyl groups residing on the surface of GO (Ting et al., 2011; Guo et al., 2009). The onset potential of the cathodic peak appeared for the hybrid (−0.3 V) is much lower than that of pristine GO (−0.7 V). Moreover, the reduction of pristine GO requires more than 15 cycles (inset to Fig. 2A), (Ting et al., 2011) whereas, that of hybrid requires only 3 cycles. These results confirm that the incorporated MWCNT significantly promotes the reduction of GO and acts as a conducting wire between the graphene sheets (Qiu et al., 2010).

3.3. Investigation of direct electrochemistry of GOx

Fig. 2B shows the cyclic voltammograms (CVs) obtained at GOx/Nf (a), ERGO/GOX/Nf (b), MWCNT/GOx/Nf (c) and ERGO–MWCNT/GOx/Nf (d) film modified GCEs in 0.1 M PBS at the scan rate of 50 mV s^{-1}. No redox peaks were observed at GOx/Nf and ERGO/GOX/Nf film modified GCEs, revealing that direct electrochemistry of GOx was not achieved on these electrodes. The CVs of MWCNT/GOx/Nf modified GCE shows a pair of redox peaks at a formal potential ($E^{\circ\prime}$) of −0.421 V with a peak to peak separation (ΔE_p) of 34 mV. Whereas, the CVs of ERGO–MWCNT/GOx/Nf film

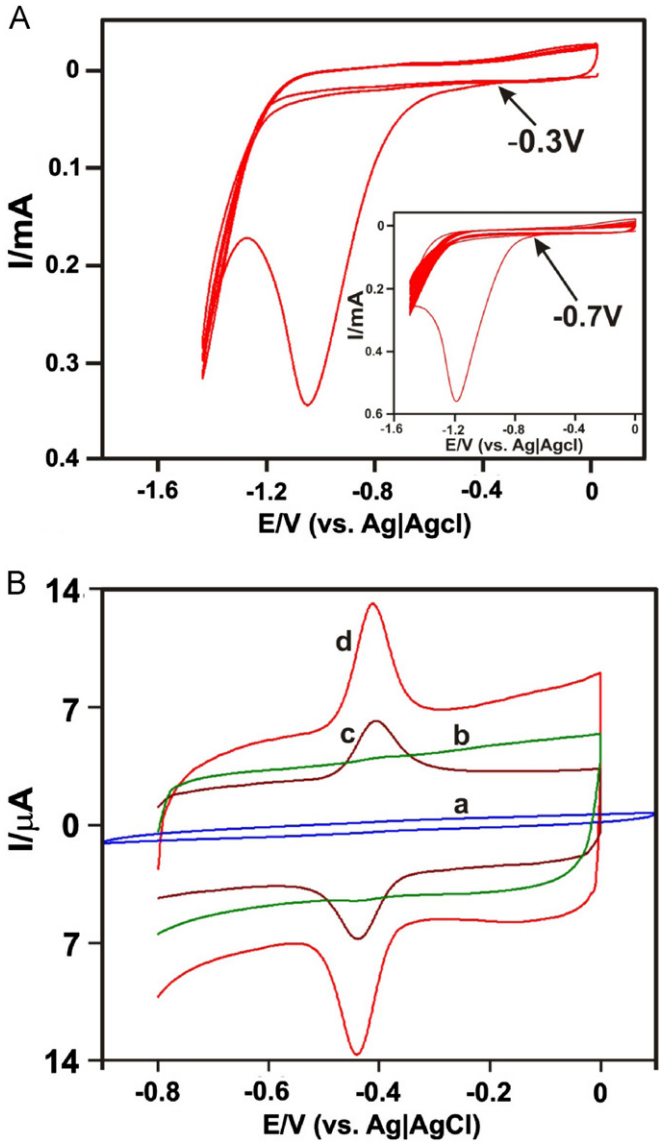

Fig. 2. (A) Electrochemical reduction of GO–MWCNT hybrid for 3 cycles in PBS (pH 5). Inset: Electrochemical reduction of pristine GO. Scan rate = 50 mV s^{-1}. (B) CVs obtained at (a) GOx/Nf, (b) ERGO/GOx/Nf, (c) MWCNT/GOx/Nf and (d) ERGO–MWCNT/GOx/Nf film modified GCEs in PBS (pH 7).

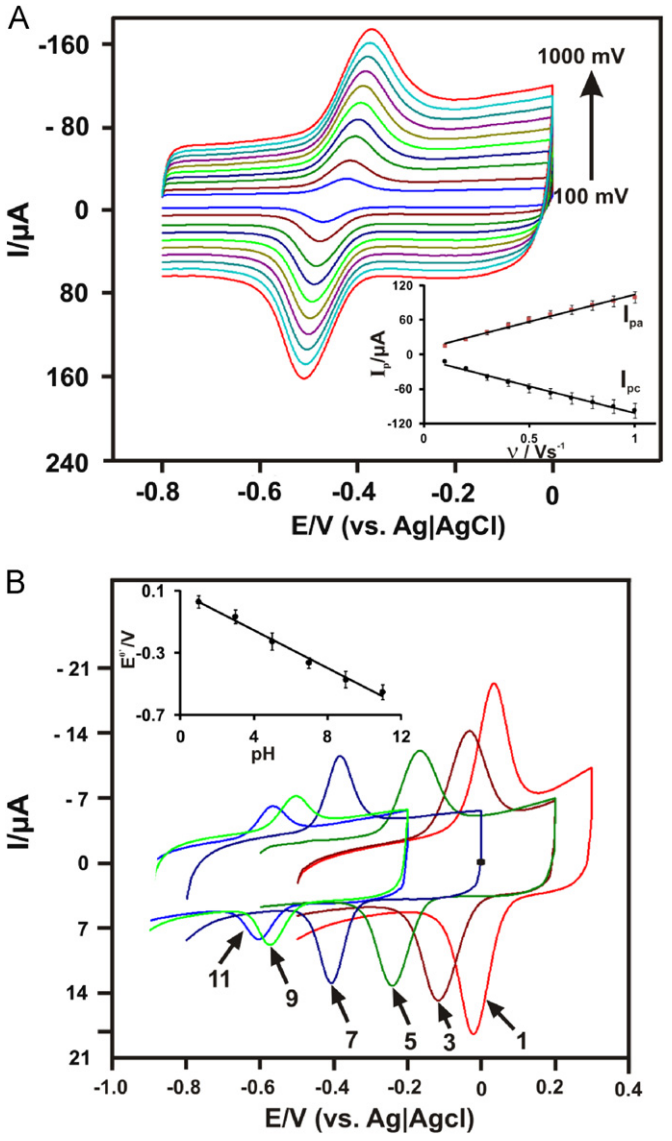

Fig. 3. (A) CVs of ERGO–MWCNT/GOx/Nf film modified GCE in PBS (pH 7) at different scan rates (from inner to outer: 0.1, 0.2, 0.3, 0.4, 0.5, 0.6, 0.7, 0.8, 0.9 and 1 V s^{-1}). Inset: Linear dependence of I_{pa} and I_{pc} on scan rates. (B) CVs obtained at ERGO–MWCNT/GOx/Nf film modified GCE in various buffer solutions (pH 1–11). Scan rate = 50 mV s^{-1}. Inset: Plot of pH vs. $E^{\circ\prime}$.

modified GCE shows a pair of well defined redox couple at $E^{\circ\prime}$ of −0.427 V with very low ΔE_p of 26 mV. Obviously, this redox couple should be ascribed to the direct electron transfer of GOx ($FAD/FADH_2$) at the ERGO–MWCNT/GOx film modified GCE. In addition, both I_{pc} and I_{pa} of ERGO–MWCNT/GOx/Nf modified GCE were 2.1 fold higher than that of MWCNT/GOx/Nf modified GCE. The enhanced redox peak currents and very low ΔE_p value indicate that GOx is highly immobilized onto the surface of ERGO–MWCNT owing to its strong interaction with ERGO–MWCNT. The plausible reason for this fascinating behavior is the large surface area and high conductivity of ERGO–MWCNT offered by the synergistic effect of two highly conducting carbon materials ERGO and MWCNT.

3.4. Effect of scan rate and pH over the direct electron transfer of GOx

The effect of scan rate on the voltammetric response of GOx was examined in deoxygenated PBS of pH 7. As shown in Fig. 3A, both I_{pa} and I_{pc} increases linearly upon increasing the scan rates from 0.1 to 1 V s^{-1}. The good linear relationship between the peak currents versus scan rates (Fig. 3A, inset) shows that the electron transfer is a surface-controlled process. Besides, the amount of electroactive enzyme on the electrode surface (Γ) can be evaluated from the slope of peak currents plotted versus scan rate by the following Eq. (1) (Bard and Faulkner, 2001)

$$I_p = n^2F^2\nu A\Gamma/4RT \quad (1)$$

where, ν (V s^{-1}) is the scan rate and A (cm^2) is the electrode surface area. The constants R, T and F have represent their usual meanings (R=8.314 J K^{-1} mol^{-1}, T=298 K, F=96485 C mol^{-1}). Assuming, the number of electrons transferred n as 2, the amount of electroactive GOx is calculated to be 3.58×10^{-10} mol cm^{-2}, which is higher than that of MWCNT/GOx/Nf modified GCE. This result proves that the large surface area of ERGO–MWCNT facilitate the high enzyme loading.

The electron transfer rate constant (k_s) between GOx and the electrode has been calculated using the Laviron Eq. (2) (Bard and

Faulkner, 2001). (For $n\Delta E_p > 0.200$ V),

$$\log K_s = \alpha\log(1-\alpha)+(1-\alpha)\log\alpha-\log(RT/nFv)-\alpha(1-\alpha)nF\Delta E_p/2.3RT \quad (2)$$

where, α is the charge transfer coefficient ($\sim$0.5) and the other parameters representing their usual meanings. The k_s value at the ERGO–MWCNT/GOx/Nf film modified GCE has been estimated to be 3.02 s^{-1} which is comparatively larger than that of boron doped CNT/GOx (1.56 s^{-1}) (Deng et al., 2008), CNT-gold colloid (1.01 s^{-1}) (Yao and Shiu, 2008), gelatin–MWCNT (1.08 s^{-1}) (Periasamy et al., 2011) and GOx–graphene–chitosan (2.83 s^{-1}) (Kang et al., 2009) modified electrodes. The larger rate constant shows that the electron shuttling between redox active sites of enzyme and the electrode surface is faster in ERGO–MWCNT. This could be attributed to the high conductivity of the ERGO–MWCNT hybrid material.

The redox couple of GOx at the ERGO–MWCNT/GOx/Nf modified film exhibit stable and well defined redox peaks over the pH range of 1 to 11(Fig. 3B).The plot of pH versus $E^{\circ\prime}$ (inset to Fig. 3B) exhibits a linear dependence over the entire pH range. The linear regression equation has been expressed as $E^{\circ\prime}$ (V)=0.088 ($\pm$1.1) (V)−0.0609 ($\pm$1.8)pH(V pH^{-1}). Besides, the slope value of −60.9 mV pH^{-1} is in close agreement with the theoretical value of −58.6 mV pH^{-1} for a reversible process involving two electrons and two protons (Periasamy et al., 2011).

Further, we demonstrated EIS experiments (Fig. S1) to investigate the immobilization of GOx and the conductivity at the various modified electrode surfaces (see the supplementary material).

3.5. Electrochemical detection of glucose based on oxygen consumption

Electrochemical detection of glucose was indirectly achieved by monitoring the oxygen consumption by the enzyme-catalyzed reaction as shown in the Eqs. (3) and (4) (Wang, 2008).

$$\text{Glucose}+O_2 \rightarrow \text{Gluconic acid}+H_2O_2 \quad (3)$$

$$O_2+4H^+ +4e^- \rightarrow 2H_2O \quad (4)$$

Fig. 4A shows the CVs of ERGO–MWCNT/GOx/Nf modified GCE in oxygen saturated PBS (pH 7) with various concentration of glucose ranging from 0.1 to 2 mM (b to d). As can be seen from Fig. 4A, the reduction current attributed to the reduction of oxygen decreases with the increase of glucose concentration. The consistent decrease in the reduction peak current illustrates the occurrence of effective oxygen reduction at the modified electrode. Thus, ERGO–MWCNT/GOx/Nf modified GCE exhibited high electrocatalytic property towards the reductive detection of the oxygen consumption which makes the indirect determination of glucose.

3.6. Electrochemical determination of glucose in the presence of mediator

Fig. 4B shows the CVs of ERGO–MWCNT/GOx/Nf modified GCE in 0.1 M PBS containing various concentration of glucose (b to m) in the presence of FMCA as the redox mediator. In the absence of glucose (a), a pair of well defined redox peaks were appeared at +0.35 V corresponding to the redox reaction of FMCA. When 0.4 mM concentration of glucose was added, a considerable increase in anodic peak current and a substantial decrease in cathodic peak current was observed. Upon, further increase in glucose concentration, the anodic peak current increased linearly with the concentration added. This result reveals that the modified electrode has great potential to catalyze the glucose oxidation effectively in the presence of FMCA. This can be explained by the Eqs. (5)–(7) (Sheng et al., 2009).

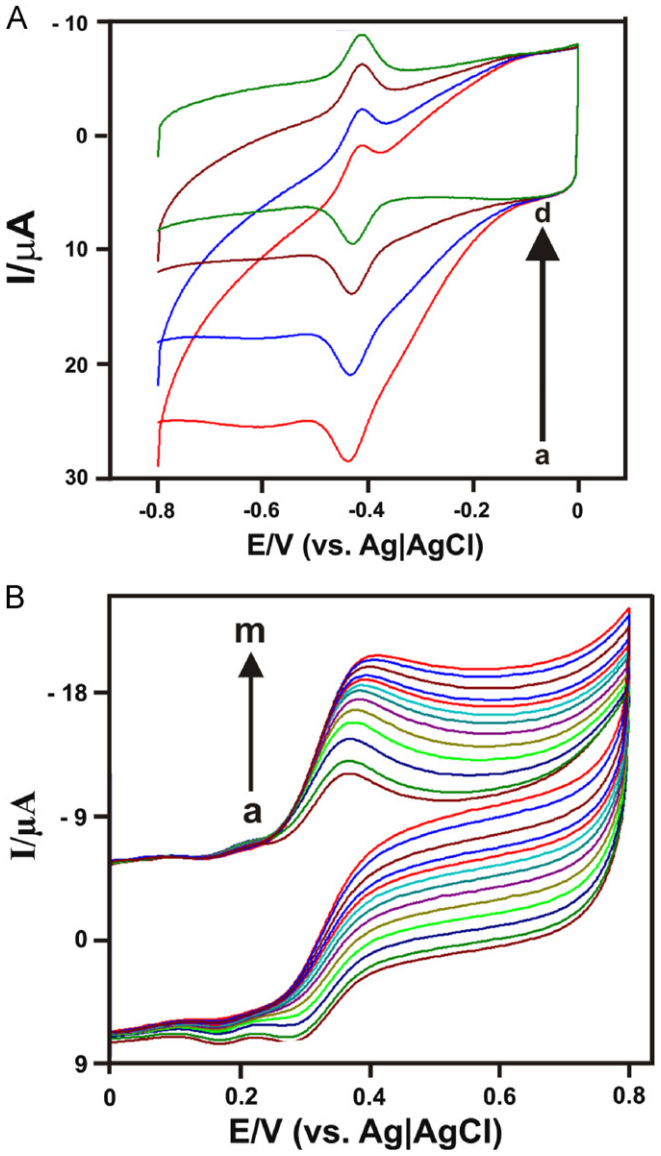

Fig. 4. (A) CVs of ERGO–MWCNT/GOx/Nf modified GCE in oxygenated PBS without glucose (a) with the additions of glucose 0.1 mM (b), 1 mM (c) and 2 mM (d). (B) CVs of ERGO–MWCNT/GOx/Nf modified GCE in 0.1 M PBS (pH 7) containing 0.5 mM FMCA without glucose (a) and with each additions of 0.4 mM glucose. ((b to m), from 0.4 to 4.8 mM).

$$\text{Glucose}+\text{GOx(FAD)} \rightarrow \text{Gluconolactone}+\text{GOx}(FADH_2) \quad (5)$$

$$\text{GOx}(FADH_2)+2\text{FMCA}^+ \rightarrow \text{GOx(FAD)}+2\text{FMCA}+2H^+ \quad (6)$$

$$2\text{FMCA} \rightarrow 2\text{FMCA}^+ +2e^- \quad (7)$$

3.7. Amperometric determination of glucose at ERGO–MWCNT/GOx/Nf modified GCE

Fig. 5A displays the amperogram obtained at ERGO–MWCNT/GOx/Nf modified rotating disc GCE at an applied electrode potential (E_{app}) of +0.35 V. 50 μM of glucose was injected sequentially at regular intervals (50 s) into the continously stirred PBS (1500 RPM) containing 0.5 mM FMCA. Well defined amperometric

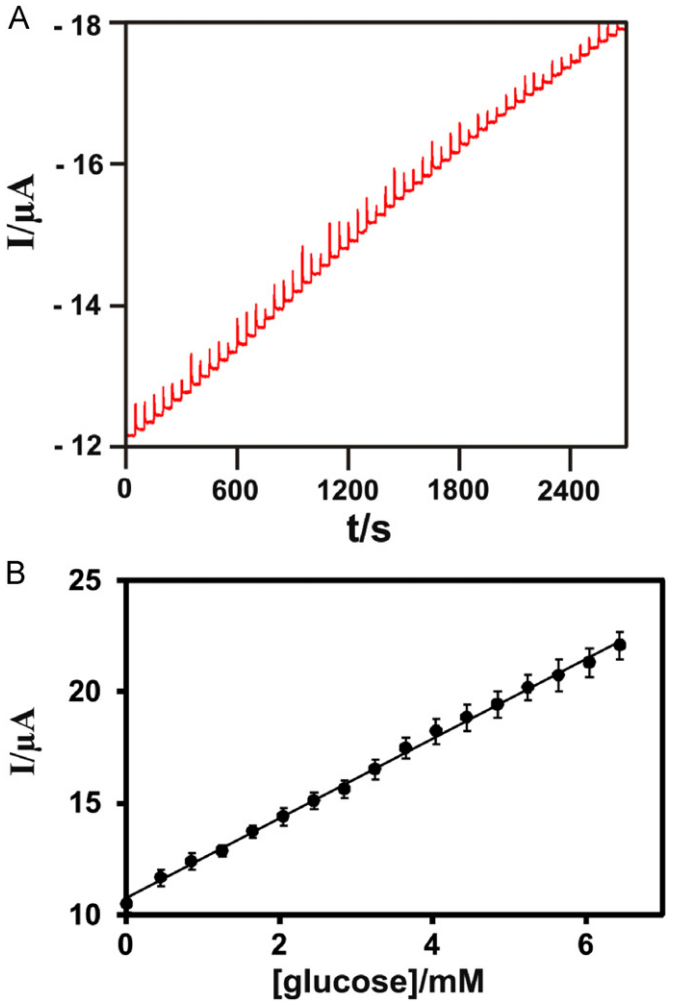

Fig. 5. (A) Amperometric *I–t* response obtained at ERGO–MWCNT/GOx/Nf modified rotating disc GCE upon successive additions of 50 μM glucose into continuously stirred PBS (pH 7) containing 0.5 mM FMCA. Rotation rate: 1500 rpm; $E_{app} = +0.35$ V. (B) Calibration plot of [glucose] vs. peak current. *Ip* (μA) = 10.36 (±) (μA) + 1.908(±)[glucose] (μA mM^{-1}). Error bars represent the standard deviation of 3 independent experiments.

responses (within 5 s) were observed for the each addition of glucose. The amperometric response current increased linearly with glucose concentrations between 10 μM and 6.5 mM, evident from the calibration plot (Fig. 5B).

The linear regression equation can be expressed as *Ip* (μA) = 10.36 (±0.052) (μA) + 1.908 (±0.087) [glucose] (μA mM^{-1}), $R^2 = 0.999$. The limit of detection (LOD) and sensitivity have been calculated to be 4.7 μM and 7.95 μA mM^{-1} cm^{-2}, respectively. The limit of detection (LOD) has been calculated using the formula, LOD = 3 s_b/S where, s_b is the standard deviation of ten blank measurements and *S* is the sensitivity (Radoi et al., 2007). The fabricated sensor exhibits a wide linear range of 0.01–6.5 mM compared with that of nitrogen-doped CNT (0.02–1.02 mM) (Deng et al., 2009), boron doped CNT (0.05–0.3 mM) (Deng et al., 2008) and nitrogen doped graphene sensors (0.1–1.1 mM) (Wang et al., 2010). Hence the proposed sensor can be quite useful to determine the blood glucose level which usually present in the range of 4.4–6.5 mM. In addition, the sensor possess very low detection limit of 4.7 μM, comparatively lower than that of MWCNT–GOx (20 μM) (Gutierrez et al., 2012) Glucose Oxidase–graphene–chitosan (20 μM) (Kang et al., 2009) and boron doped CNT (10 μM) (Deng et al., 2008). Therefore, the proposed sensor shows better performance compared with other glucose sensors. Moreover, a comparison of analytical parameters of ERGO–MWCNT/GOx/Nf modified GCE with other mediated glucose sensors has been made and given in Table S1.

3.8. Real sample analysis

The practicality of the ERGO–MWCNT/GOx/Nf modified electrode has been assessed by the glucose determination in the human blood serum and spiked urine samples. Human blood serum was collected from a healthy man and the glucose concentration was pre-determined to be 4.094 mM by ROCHE COBAS C 111 ANALYZER (photometric analysis). To determine the glucose content of the serum by using the proposed sensor, 2 mL of the blood serum was diluted to 10 mL by adding PBS (pH 7) (Unnikrishnan et al., 2012). The experiment has been performed using ERGO–MWCNT/GOx/Nf modified GCE with the diluted serum following the similar experimental conditions as of Section 3.8. We adopt standard addition method to determine the concentration of glucose and it was found to be to be 4.316 mM with an acceptable RSD of 3.7 for three measurements. The results showed that the concentration determined by the proposed sensor is in good agreement with the commercial analyzer. Therefore the fabricated glucose sensor can be useful for the efficient determination of glucose present in the human blood serum samples.

Furthermore, spiked human urine sample also studied to prove the practical application of the fabricated sensor towards glucose determination. Glucose was spiked into the urine samples collected from a healthy man and the samples were diluted in the ratio of 1:100 with 0.1 M PBS (pH 7). The spiked samples were analyzed using ERGO–MWCNT/GOx/Nf modified GCE by amperometry. The comparison of the spiked values and the determined values were listed in Table 1. The added glucose shows the good recoveries from 97.6% to 102.5%. The good recoveries achieved in the spiked urine samples reveal the appreciable practicality of the sensor. Thus, the accurate glucose determination in human blood serum and good recoveries achieved in spiked urine samples revealed the excellent practical feasibility of the fabricated ERGO–MWCNT composite film based sensor towards the determination of glucose.

3.9. Repeatability, reproducibility and stability studies

The repeatability and reproducibility of the sensor has been assessed by CV studies. CVs were recorded in 0.1 M PBS (pH 7) at the scan rate of 50 mV s^{-1} in the presence of 0.5 mM FMCA towards each 3 mM glucose addition.The fabricated sensor shows good repeatability with a relative standard deviation (R.S.D) of 3.95% for 10 successive measurements. Morover, it exhibits a good reproducibility with an R.S.D of 2.5% for 7 individual measurements.

The stability of ERGO–MWCNT/GOx/Nf film has been studied by recording consecutive CVs in PBS (pH 7). About 94% of the background current was retained even after 100 successive cycles. In order to determine the storage stability, ERGO–MWCNT/

Table 1
Determination of glucose in urine samples at ERGO–MWCNT/GOx/Nf film modified GCE.

Samples	Added	Found	[a]RSD (%)	Recovery
1	2.0 mM	2.05 mM	3.1	102.5
2	3.0 mM	2.93 mM	2.6	97.66
3	80 μM	78.7 μM	3.0	98.37
4	100 μM	101.5 μM	2.2	101.5

[a] Relative standard deviation (RSD) of 4 measurements.

GOx/Nf film modified GCE was stored in PBS at 4 °C and CV background currents were monitored. The modified film retained its 90% peak current even after one month. Thus, the above results proved the excellent stability of the modified film and strong interaction of GOx to the hybrid. Afterwards, we attempt to investigate the operational stability of the modified film in the presence of 5 mM glucose into continuously stirred (1500 RPM) PBS containing FMCA (E_{app} of +0.35 V). Even after continously operated for 3000 s, the response current decreased only by 7%, indicating the excellent operational stability of the modified film. Thus, both storage and operational stabiliies are appreciable owing to the stability of the ERGO–MWCNT hybrid material.

4. Conclusions

We achieved the direct electrochemistry for GOx by employing ERGO–MWCNT hybrid material. The preperation of the hybrid material is simple, efficient, and green technique.The modified electrode exhibited high electrocatalytic activity towards glucose determination via oxygen consumption and in presence of mediator. The fabricated biosensor possesses excellent analytical performances with appreciable storage and operational stabilities. The real sample studies were performed in human blood serum and urine samples. The good recoveries achieved were making the sensor suitable for the practical applications. As, a future perspective the fabricated GOx based modified electrode will be used for the biofuel cell applications.

Acknowledgement

This work was supported by the National Science Council and the Ministry of Education of Taiwan (Republic of China). The authors would like to thank, Dr. Arun Prakash Periasamy and Mr. Boopathi Subramani for their valuable help throughout this project.

Appendix A. Supporting information

Supplementary data associated with this article can be found in the online version at 10.1016/j.bios.2012.08.045.

References

Bard, A.J., Faulkner, L.R., 2001. Wiley, New York.
Chen, D., Tang, L., Li, J., 2010. Chemical Society Reviews 39, 3157–3180.
Deng, C., Chen, J., Chen, X., Xiao, C., Nie, L., Yao, S., 2008. Biosensors and Bioelectronics 23, 1272–1277.
Deng, S., Jian, G., Lei, J., Hu, Z., Ju, H., 2009. Biosensors and Bioelectronics 25, 373–377.
Dreyer, D.R., Park, S., Bielawski, C.W., Ruoff, R.S., 2010. Chemical Society Reviews 39, 228–240.
Gao, X., Jang, J., Nagase, S., 2010. Journal of Physical Chemistry C 114, 832–842.
Geim, A.K., Novoselov, K.S., 2007. Nature Materials 6, 183–191.
Guo, H.L., Wang, X.F., Qian, Q.Y., Wang, F.B., Xia, X.H., 2009. ACS Nano 3, 2653–2659.
Gutierrez, F., Rubianes, M.D., Rivas, G.A., 2012. Sensors and Actuators B: Chemical 161, 191–197.
Hummers, W.S., Offeman, R.E., 1958. Journal of the American Chemical Society 80, 1339.
Jacobs, C.B., Peairs, M.J., Venton, B.J., 2010. Analytica Chimica Acta 662, 105–127.
Kachoosangi, R.T., Musameh, M.M., Yousef, I.A., Yousef, J.M., Kanan, S.M., Xiao, L., Kang, X., Wang, J., Wu, H., Aksay, I.A., Liu, J., Lin, Y., 2009. Biosensors and Bioelectronics 25, 901–905.
Kang, Y., Taton, T.A., 2003. Journal of the American Chemical Society 125, 5650–5651.
Kang, X., Wang, J., Wu, H., Aksay, I.A., Liu, J., Lin, Y., 2009. Biosensors and Bioelectronics 25, 901–905.
Mani, V., Periasamy, A.P., Chen, S.-M., 2012. Electrochemistry Communications 17, 75–78.
Periasamy, A.P., Chang, Y.-J., Chen, S.-M., 2011. Bioelectrochemistry 80, 14–120.
Pumera, M., Ambrosi, A., Bonanni, A., Chng, E.L.K., Poh, H.L., 2010. TRAC Trends in Analytical Chemistry 29, 954–965.
Qiu, J.-D., Huang, J., Liang, R.-P., 2012. Sensors and Actuators B: Chemical 160, 287–294.
Qiu, L., Yang, X., Gou, X., Yang, W., Ma, Z.F., Wallace, G.G., Li, D., 2010. Chemistry A European Journal 16, 10653–10658.
Radoi, A., Compagnone, D., Devic, E., Palleschi, G., 2007. Sensors and Actuators B: Chemical 121, 501–506.
Ramesha, G.K., Sampath, S., 2007. Electroanalysis 19, 2472–2478.
Shan, C., Yang, H., Song, J., Han, D., Ivaska, A., Niu, L., 2009. Analytical Chemistry 81, 2378–2382.
Sheng, Q., Luo, K., Li, L., Zheng, J., 2009. Bioelectrochemistry 74, 246–253.
Ting, S.W., Periasamy, A.P., Chen, S.-M., Saraswathi, R., 2011. International Journal of Electrochemical Science 6, 4438–4453.
Unnikrishnan, B., Palanisamy, S., Chen, S.-M., 2012. Biosensors and Bioelectronics.
Wang, Y., Shao, Y., Matson, D.W., Li, J., Lin, Y., 2010. ACS Nano 4, 1790–1798.
Wang, J., 2005. Electroanalysis 17, 7–14.
Wang, J., 2008. Chemical Reviews 108, 814–825.
Xiao, C., Chu, X., Wu, B., Pang, H., Zhang, X., Chen, J., 2010. Talanta 80, 1719–1724.
Yao, Y.-L., Shiu, K.-K., 2008. Electroanalysis 20, 1542–1548.
Yoo, E., Kim, J., Hosono, E., Zhou, H.-S., Kudo, T., Honma, I., 2008. Nano Letters 8, 2277–2282.
Zhang, C., Ren, L., Wang, X., Liu, T., 2010. Journal of Physical Chemistry C 114, 11435–11440.
Zhou, K., Zhu, Y., Yang, X., Li, C., 2010. Electroanalysis 22, 259–264.